



Degradation of carbamazepine by Fe(II)-activated persulfate process

Y.F. Rao ^{a,*}, Liang Qu ^a, Haisong Yang ^a, W. Chu ^{b,*}

^a Department of Environmental Science and Engineering, Xi'an Jiaotong University, Xi'an 710049, China

^b Department of Civil and Environmental Engineering, The Hong Kong Polytechnic University, Hung Hom, Kowloon, Hong Kong



HIGHLIGHTS

- Oxidative degradation of carbamazepine by Fe(II)/persulfate process is reported. CBZ degradation rate depends on pH value and the ratio of $[Fe^{2+}]:[S_2O_8^{2-}]:[CBZ]$. The anions NO_3^- , SO_4^{2-} and $H_2PO_4^-$ caused a negative effect on CBZ degradation.
- The higher the Cl^- concentration, the faster the CBZ decay rate.
- The presence of Cl^- influences the evolution profiles of various intermediates.

ARTICLE INFO

Article history:

Received 1 September 2013

Received in revised form

30 December 2013

Accepted 6 January 2014

Available online 14 January 2014

Keywords:

Carbamazepine

Kinetics

Sulfate radicals

Decay pathways

ABSTRACT

Experimental studies were conducted to investigate the oxidative degradation of carbamazepine (CBZ), one of the most frequently detected pharmaceuticals in various waters, by Fe(II)-activated persulfate process. Results show that the $Fe^{2+}/S_2O_8^{2-}$ process is very effective for the elimination of CBZ and characterized by a two-stage kinetics (a rapid initial decay followed by a retardation stage). CBZ degradation reaction was observed to be pH dependent and the optimum pH is 3.0 in the range of 2.00–7.87. The concentration of Fe^{2+} and $S_2O_8^{2-}$ exhibited a noticeable influence on CBZ removal efficiency, where $[S_2O_8^{2-}]$ exerted more significant effects than that of $[Fe^{2+}]$. The optimal molar ratio of CBZ, Fe^{2+} , and $S_2O_8^{2-}$ is found to be 1:5:40. The effect of various inorganic anions on CBZ removal was also evaluated under the optimal conditions. The anions NO_3^- , SO_4^{2-} and $H_2PO_4^-$ caused a negative effect on the performance of this process, while Cl^- interestingly accelerated CBZ degradation. The higher the Cl^- concentration, the faster the CBZ decay rate. The intermediates were identified during CBZ degradation with and without the presence of Cl^- . The evolution of intermediates for these two scenarios was compared. The decay pathways of CBZ were proposed accordingly.

© 2014 Elsevier B.V. All rights reserved.

1. Introduction

Pharmaceuticals, as emerging pollutants in aquatic environments, have received increasing concerns recently. The production of drugs has been estimated in several hundred tons per year [1]. Most pharmaceuticals are not completely degraded after application. Thus, the pharmaceutical metabolites and some unchanged forms of these compounds are excreted and continuously enter the ecosystem, which led to various pharmaceuticals being detected in aquatic environment. In addition, the inappropriate disposal of pharmaceuticals is believed to make an important contribution to the widespread occurrence of pharmaceuticals in the environment [2].

Carbamazepine (CBZ) is a typical compound used for the treatment of seizure disorders, relief of neuralgia, and a wide variety of psychiatric disorders. The worldwide consumption of CBZ is estimated to be 1014 t per year [2] and its annual usage ranks the second among all the antiepileptic drugs in China [3]. CBZ is one of the most frequently detected pharmaceuticals in various waters due to its low biodegradability and persistent nature in wastewater. CBZ has been detected in WWTP effluents at concentrations up to 6.3 μ g/L [4,5]. The CBZ concentration was found to be 3.09 μ g/L, 610 ng/L and 30 ng/L in surface water [6], groundwater [7], and drinking water [8], respectively. CBZ has been evaluated as toxic to aquatic life including bacteria, algae, invertebrates, and fish [9,10].

Advanced oxidation processes (AOPs) have been considered to be a promising technology to treat water and wastewater containing toxic and non-biodegradable pollutants due to the generation of highly reactive radicals. Several AOPs such as photocatalysis [11,12], ozonation [13], US/Fenton [14], UV/ H_2O_2 and UV/Fenton [15] have been evaluated for the elimination of CBZ. In recent years, sulfate radicals-based oxidation technologies have attracted increasing interests [16–18]. Persulfate anion ($S_2O_8^{2-}$, PS) is a

* Corresponding authors at: Xi'an Jiaotong University, Department of Environmental Science and Engineering, No.28, Xianning West Road, Xi'an 710049, China. Tel.: +8613629200175.

E-mail addresses: yfrao@mail.xjtu.edu.cn, ryf99@126.com (Y.F. Rao), wei.chu@polyu.edu.hk (W. Chu).

strong oxidant with a redox potential of 2.01 V. Persulfate has been considered to be a promising choice for clean-up applications due to the ease of storage and transport, stability, pH-independence and low cost [17]. $S_2O_8^{2-}$ can be activated to generate sulfate radicals ($SO_4^{\bullet-}$) with higher redox potential of 2.6–3.1 V [19] either by the homolysis of the peroxide bond using heat [20,21], ultrasound [22], microwave [23] or light [17], or by a redox reaction process (Fenton-like) [24,25]. Compared to hydroxyl radicals, sulfate radicals are more selective and demonstrate higher standard reduction potential at neutral pH [16]. Sulfate radicals have been proved more efficient than hydroxyl radicals for the degradation of several compounds such as 2,4-dichlorophenol, atrazine, and naphthalene [26].

This contribution made the first attempt to examine the degradation of CBZ by Fe(II)-activated persulfate process. Effects of some critical parameters, including Fe(II), oxidant concentration, solution pH, and inorganic anions on CBZ degradation efficiency were investigated. This work also examined the intermediates and the evolution profiles of intermediates during CBZ decay by Fe(II)/PS process with and without the presence of chloride.

2. Materials and methods

2.1. Chemicals

The probe CBZ was purchased from Tokyo Chemical Industry. Carbamazepine 10,11-epoxide was obtained from Fluka. Potassium peroxydisulfate ($K_2S_2O_8$), ferrous sulfate ($FeSO_4 \cdot 7H_2O$), sodium chloride ($NaCl$), sodium nitrate ($NaNO_3$), sodium sulfate (Na_2SO_4), and sodium dihydrogen phosphate (NaH_2PO_4) were purchased from Sigma-Aldrich. All chemicals are in analytic purity and all solvents are HPLC grade and used without further purification. All aqueous solutions were prepared in distilled and deionized water (DDW) with a resistivity of 18.0 MΩ from a Millipore Waters Milli-Q water purification system.

2.2. Experimental procedures

The degradation tests were performed in 250 mL batch reactors. CBZ stock solution (0.1 mM) was prepared in DDW and specific aliquots of the solution were added into the reactors to attain a pre-determined initial concentration. The ferrous solution was freshly prepared before each test to minimize variations in concentration caused by precipitation and oxidation of ferrous solution. The Fe(II) solution was prepared in degassed H_2SO_4 solution at pH 2.5 to prevent Fe(II) from precipitation and/or oxidation. The reactions were initiated by pipetting appropriate amounts of Fe(II) and PS into the reactor to achieve the predefined molar ratios of CBZ:Fe(II):PS. The initial volume of the reaction solution was fixed at 100 mL with mechanic stirring during the reaction to ensure a thorough mixing. The pH values were adjusted with 0.01 M sulfuric acid and/or 0.01 M sodium hydroxide whenever required. At predetermined time intervals, the sample aliquots were withdrawn from the reactor and sodium thiosulfate [27] was added to quench the reaction. The solution was then analyzed by high performance liquid chromatography (HPLC) to quantify the remaining CBZ. All experiments were carried out in duplicate and the error is less than 3.0%.

2.3. Analytical procedures

The remaining CBZ after reaction was determined by HPLC, which was comprised of a Waters 515 HPLC pump, Waters 2489 Dual λ Absorbance Detector, and a RESTEK C18 column (pinnacle DB, 250 × 4.6 mm, and 5 μm particle size). The maximum adsorption wavelength (λ_{max}) was selected as 210 nm for CBZ. A mixture of 60% acetonitrile and 40% water was used as the mobile phase

running at a flow rate of 0.8 mL/min. The concentration of Fe^{2+} was determined colorimetrically using an UV-vis spectrophotometer at 510 nm after adding 1,10-phenanthroline to form a colored complex of Fe^{2+} -phenanthroline.

The identification of intermediates was carried out at an initial CBZ concentration of 0.15 mM. A Thermo Quest Finnigan LCQ Duo Mass Spectrometer system was used with RESTEK C18 column (pinnacle DB, 250 × 4.6 mm, and 5 μm particle size). The LC detection system consisted of a photodiode array UV-vis detector. The reaction intermediates were identified by using LC-ESI-MS/MS operating at a positive mode with collision energy ranging from 25% to 35%. A gradient method with a flow rate of 0.8 mL/min was used with a mobile phase containing A (5 mM ammonium acetate at pH 4.6) and B (100% acetonitrile). Component A was maintained at 85% during the first 2 min, then B was steadily increased from 15% to 85% in the next 34 min. Finally, the mobile phase returned to the initial composition until the end of the run.

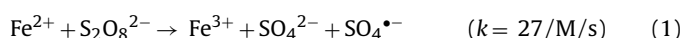
The reaction intermediates were also identified by SPME (Solid phase microextraction)/GC/MS. SPME analyses were performed using a PAL Combi-xt autosampler (CTC, Switzerland). A 65 μm polydimethylsiloxane/divinylbenzene (PDMS/DVB) SPME fiber (Supelco, Seelze, Germany) was exposed directly into the liquid sample. The aqueous solution was agitated in the incubator (incubation time 1 min, temperature 40 °C) at a speed of 250 rpm. The agitator on and off times were 60 s and 1 s, respectively. After extraction, the compounds were thermally desorbed for 300 s in the GC injector. After desorption, the fiber was reconditioned in an externally heated needle heater under a light helium flow at a temperature of 270 °C. The GC system (TRACE GC ULTRA, Thermo SCIENTIFIC) was equipped with a 30 m HP-5MS capillary column (Agilent Technologies, Santa Clara, US) with an i.d. of 250 μm and a film thickness of 0.25 μm. Helium 5.0 served as the carrier gas. The GC oven temperature program was as follows: initial temperature 50 °C for 2 min, followed by heating at 10 °C min⁻¹ to 250 °C and held at 250 °C for 1 min, then at 5 °C min⁻¹ from 250 °C to 280 °C, and finally held for 1 min at 280 °C. Thermo SCIENTIFIC ISQ MS was run at EI mode. MS transfer line and ion source temperature were set at 300 °C and 250 °C, respectively.

Total organic carbon (TOC) concentration was measured by a TOC analyzer (ShimadzuTOC-5000A). The concentration of persulfate ion was determined by spectrophotometric method [28].

3. Results and discussion

3.1. Kinetics of CBZ degradation

CBZ decay by Fe(II)/PS process and the associated sole components is presented in Fig. 1. It can be seen that sole-PS could not oxidize CBZ and there was no change in CBZ concentration when Fe^{2+} was introduced into CBZ solution. The latter indicates no complex formation between Fe^{2+} and CBZ. As also demonstrated in Fig. 1, the degradation of CBZ by $Fe^{2+}/S_2O_8^{2-}$ is characterized by a two-stage kinetics, where a faster initial decay followed by a retardation stage. At the initial stage, fast reaction between Fe^{2+} and $S_2O_8^{2-}$ at high concentration (0.25 mM) led to a rapid generation of sulfate radicals (The production rate of sulfate radicals is 1.69×10^{-3} mM/s based on Eq. (1)). Two minutes later, only 0.0325 mM Fe^{2+} ions remained in the solution (data not shown); as a result, the generation of sulfate radicals slowed down. Furthermore, the intermediates generated during the reaction competed with CBZ for sulfate radicals, which also resulted in a retarded CBZ decay at the second stage.



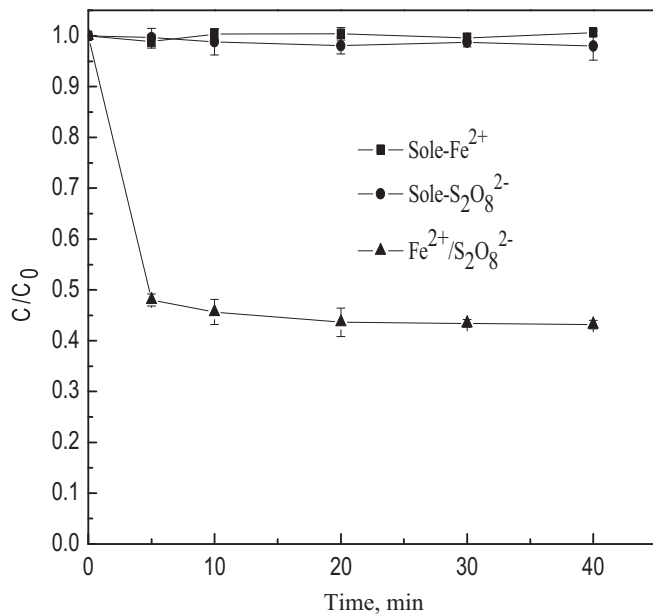
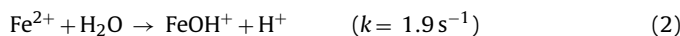


Fig. 1. CBZ degradation under different reaction conditions. Experimental conditions: $[CBZ]_0 = 0.025 \text{ mM}$, $[Fe^{2+}]_0 = 0.25 \text{ mM}$, $[S_2O_8^{2-}] = 0.25 \text{ mM}$, initial pH is 3.0.

3.2. Effect of initial pH levels

The effects of initial pH levels ranging from 2.00 to 7.87 on CBZ degradation were examined in this study (see Fig. 2a), where the pH levels exerted significant influence on the performance in $Fe^{2+}/S_2O_8^{2-}$ system. The fastest initial decay rate of CBZ was observed at pH 4.22. However, CBZ decay rate at the second-stage is slightly slower at pH 4.22 than that at pH 3.0 due to the formation of iron precipitation. The initial decay rate of CBZ was slower at pH 2.00 than that at pH 3.00, which can be rationalized by two explanations. First, complex $(Fe(H_2O))^{2+}$ is formed at low pH levels [29], leading to a deficient free Fe^{2+} for activating PS ions in the solution, and then fewer sulfate radicals. Fig. 2b shows the degradation rate of PS was slower at pH 2.00 than that at pH 3.00 and 4.22, which justified the first explanation. Second, CBZ has a pK_{a1} of 2.3 related to the protonation of the NH_2 group and pK_{a2} of 13.9 related to the deprotonation of the amino group [30]; indicating nearly half of CBZ could exist in a protonated form at pH 2.00. The electrophilic property of sulfate radical led to a lower reactivity towards CBZ carrying positive charge.

As also shown in Fig. 2a, CBZ decay rate dropped rapidly with the increase of the initial pH level (from 4.22 to 7.87). It was known that the amount of free Fe^{2+} could decline due to the formation of Fe^{2+} complexes when the pH level is higher than 4.0, as described by Eq. (3):



The further increase of pH level could cause the generation of $Fe(OH)_2$. Both $FeOH^+$ and $Fe(OH)_2$ have much lower catalytic activity towards PS ions as indicated in Fig. 2b, therefore, producing fewer sulfate radicals. In addition, the formation of precipitation was observed when the pH level is higher than 4.0, which is believed to be ferric hydroxide complexes such as $FeOH^{2+}$, $Fe_2(OH)_4^{4+}$, $Fe(OH)^{2+}$, $Fe(OH)_3$ and $Fe(OH)_4^-$. The precipitation of $Fe(OH)_2$ was not observed due to the solubility product of $Fe(OH)_2$ being 1.64×10^{-14} . These ferric hydroxide complexes have very low efficiency to activate PS nor to generate sulfate radicals. As demonstrated in Fig. 2a, the degradation of CBZ was no longer observed at pH 7.87, suggesting the deficiency of Fe^{2+} as an activator. The concentration of PS ions increased at pH 7.87, which is due to the

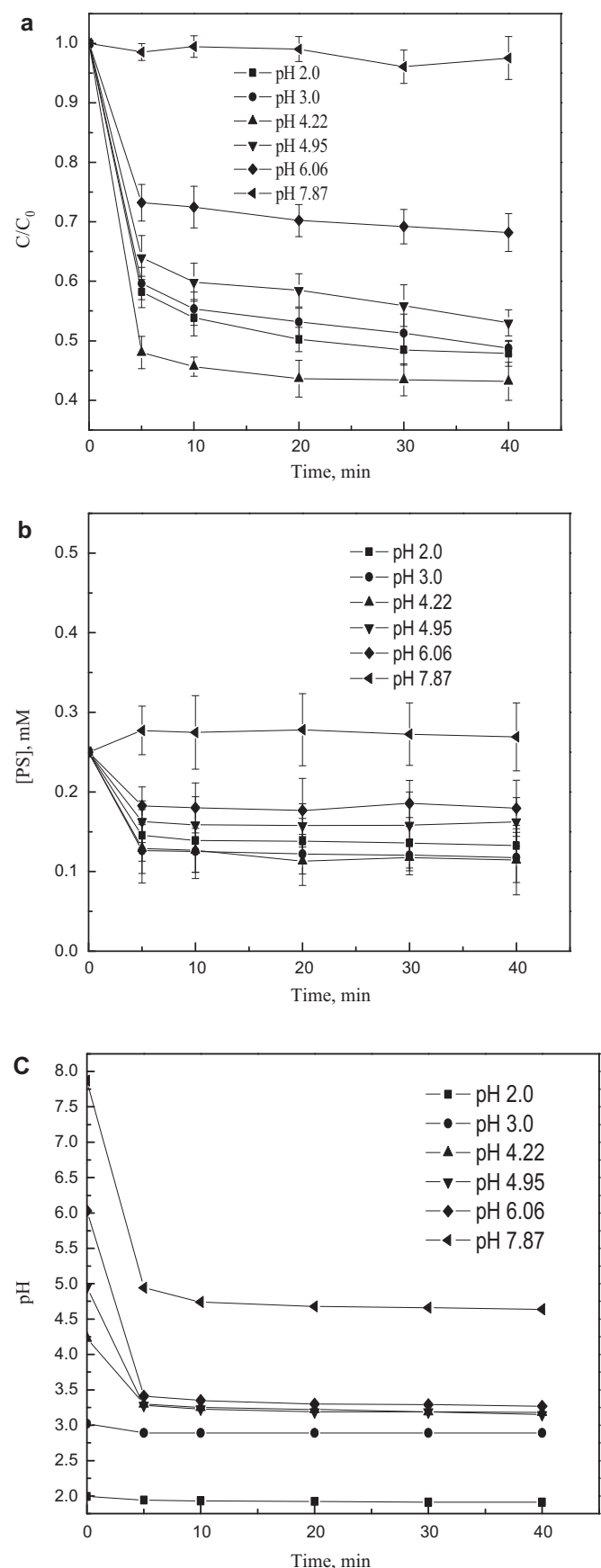


Fig. 2. (a) Effect of initial pH level on CBZ degradation; (b) time course of PS during CBZ degradation reaction; (c) time course of pH levels during CBZ degradation reaction. Experimental conditions: $[CBZ]_0 = 0.025 \text{ mM}$, $[Fe^{2+}]_0 = 0.25 \text{ mM}$, $[S_2O_8^{2-}] = 0.25 \text{ mM}$.

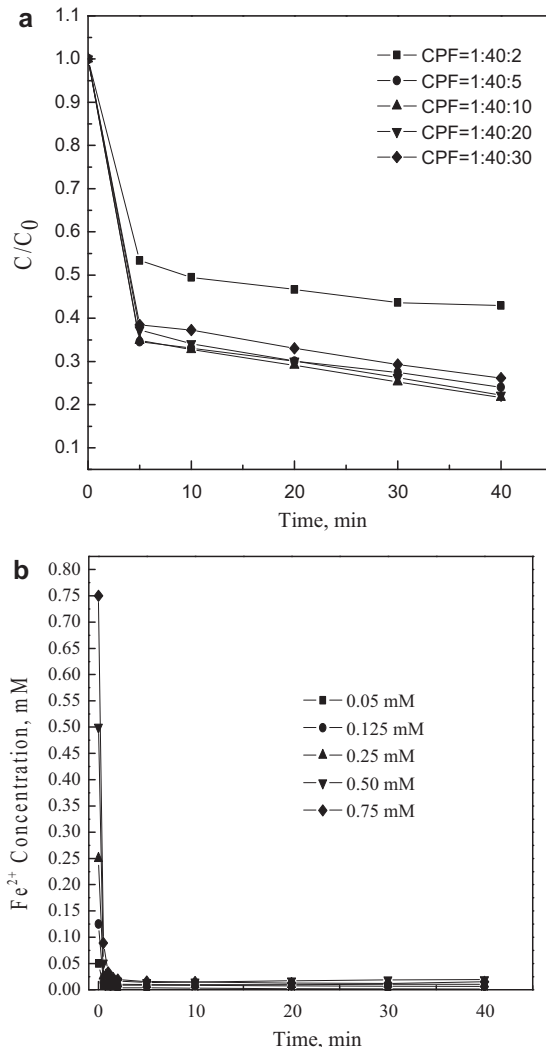
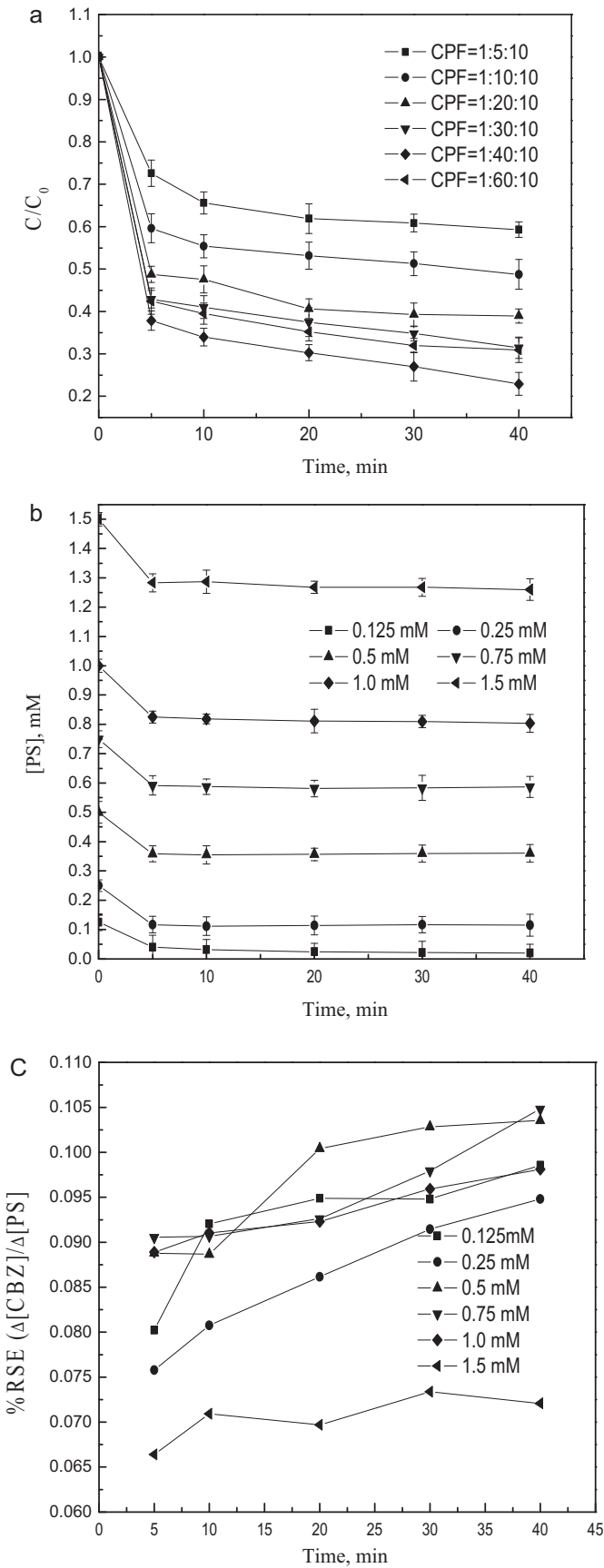


Fig. 4. (a) Effect of Fe^{2+} concentration on CBZ degradation; (b) variation of Fe^{2+} concentration over time. Experimental conditions: $[CBZ]_0 = 0.025\text{ mM}$, $[S_2O_8^{2-}] = 1\text{ mM}$, initial pH is 3.0.

generation of precipitant affecting the measurement of PS concentration by spectrophotometric method. The variation of pH value during the reaction was shown at in Fig. 2C. The pH level slightly decreased during CBZ decay reaction when the initial pH was 2.00 and 3.00. The pH level declined significantly at the initial stage of the reaction and remained stable at the second stage (after 5 min) when the initial pH was above 4.22.

3.3. Effect of initial PS concentration on CBZ degradation

PS concentration is a critical parameter as the source of sulfate radicals in $Fe^{2+}/S_2O_8^{2-}$ process. The influence of PS dosage on CBZ decay was evaluated by varying PS/ Fe^{2+} ratios from 1:2 to 6:1 with Fe^{2+} concentration fixed at 0.25 mM. Fig. 3a shows the increasing ratio of PS/ Fe^{2+} from 1:2 to 4:1 leading to an enhancement in CBZ removal efficiency from 41% to 78% in 40 min. The further increase of PS dosage, however resulted in a decline in CBZ removal. Similar phenomenon has been observed in the degradation of trichloroethane (TCE) by ultrasound-activated persulfate process where the overdose of PS resulted in the decrease of TCE degradation rate [22]. The degradation profile of PS is illustrated in Fig. 3b. Complete consumption of PS was not observed after 40 min of reaction even for PS/ Fe^{2+} ratio of 1:2. In order to better optimize

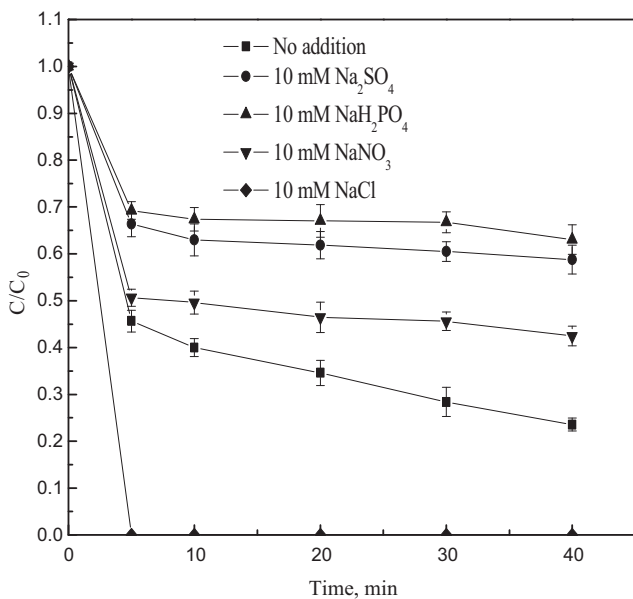


Fig. 5. Effect of inorganic anions on CBZ degradation. Experimental conditions: $[\text{CBZ}]_0 = 0.025\text{ mM}$, $[\text{Fe}^{2+}]_0 = 0.125\text{ mM}$, $[\text{S}_2\text{O}_8^{2-}] = 1\text{ mM}$, initial pH is 3.0.

this process, the reaction stoichiometric efficiency (RSE) was calculated for all PS concentrations used at different reaction time (5–40 min) as indicated in Fig. 3c. RSE averages ranged between 6.64% and 10.48%. The highest RSE was observed at 0.5 mM of PS concentration at most reaction time while the lowest RSE was noticed for the highest PS load.

3.4. Effect of initial Fe^{2+} concentration

Fig. 4 shows the influence of Fe^{2+} concentration on CBZ degradation with PS concentration fixed at 1 mM. CBZ decay was slow if the $[\text{Fe}^{2+}]$ was low at a $[\text{PS}]/[\text{Fe}^{2+}]$ ratio of 40:2. The increase of $[\text{Fe}^{2+}]$ would surely accelerate the CBZ degradation, but the differences contributed by varying $[\text{Fe}^{2+}]$ with ratios ranging from 40:5 to 40:30 was not impressive. Higher dosage of Fe^{2+} ions could improve the

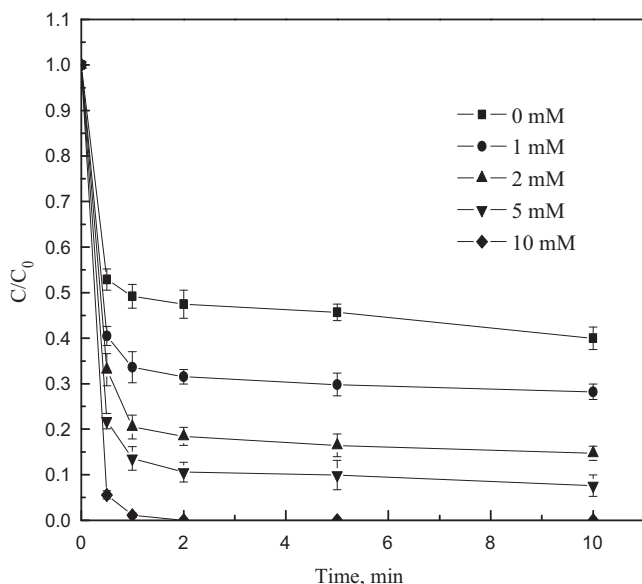


Fig. 6. Effect of Cl^- concentration on CBZ decay by $\text{Fe}^{2+}/\text{S}_2\text{O}_8^{2-}$ process. Experimental conditions: $[\text{CBZ}]_0 = 0.025\text{ mM}$, $[\text{Fe}^{2+}]_0 = 0.125\text{ mM}$, $[\text{S}_2\text{O}_8^{2-}] = 1\text{ mM}$, initial pH is 3.0.

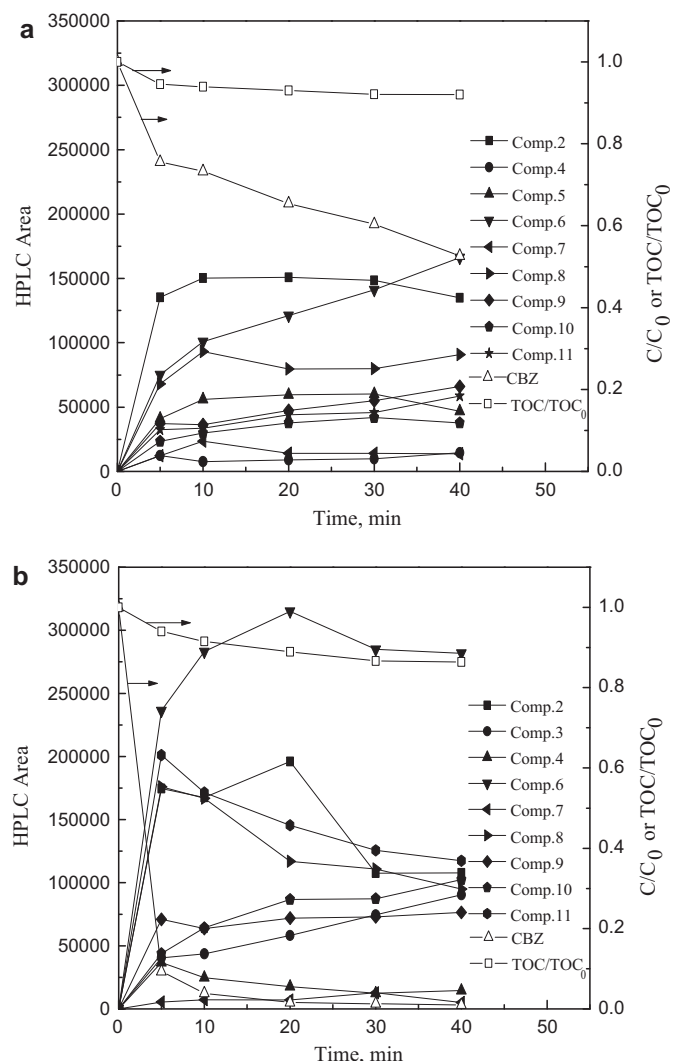
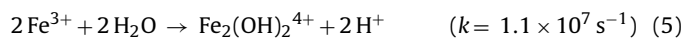
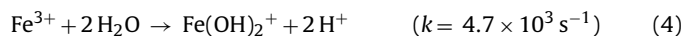
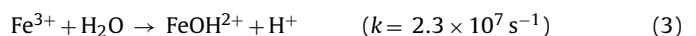


Fig. 7. (a) Evolution profiles of CBZ, TOC and intermediates in the absence of Cl^- . (b) Evolution profiles of CBZ, TOC and intermediates in the presence of Cl^- . Experimental conditions: $[\text{CBZ}]_0 = 0.15\text{ mM}$, $[\text{Fe}^{2+}]_0 = 0.75\text{ mM}$, $[\text{S}_2\text{O}_8^{2-}] = 6\text{ mM}$, $[\text{Cl}^-] = 10\text{ mM}$, initial pH is 3.0.

generation rate of sulfate radicals which accelerated the decomposition of CBZ. However, Fe^{2+} can also act as an effective scavenger of sulfate radicals. When $[\text{Fe}^{2+}]/[\text{PS}]$ is higher than 5:40, a balance between the generation and consumption of sulfate radicals was likely achieved, and the CBZ decay rate leveled off.

The variation of $[\text{Fe}^{2+}]$ was monitored during the reaction with different initial $[\text{Fe}^{2+}]$ ranging from 0.05 to 0.75 mM. As shown in Fig. 4b, Fe^{2+} was consumed rapidly and the concentration reduced sharply in the first 30 s in all tests. It was believed that Fe^{2+} was oxidized to Fe^{3+} which then transformed to various Ferric oxyhydroxides through hydrolysis. The formations of ferric oxyhydroxides are described in the following Eqs. (3)–(5) [31]:



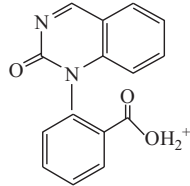
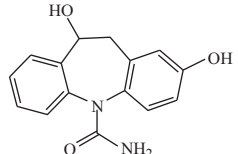
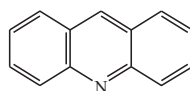
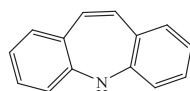
At pH 3, FeOH^{2+} is the dominant species in the solution [31]. It was found that Fe^{3+} , FeOH^{2+} and $\text{Fe}(\text{OH})_2^+$ have lower efficiency to activate PS to create sulfate radicals. This was confirmed by an independent test, where CBZ was decayed by $\text{Fe}^{3+}/\text{S}_2\text{O}_8^{2-}$, with a

Table 1

Intermediates and products detected by LC-MS/MS and SPME/GC/MS during CBZ degradation by $\text{Fe}^{2+}/\text{S}_2\text{O}_8^{2-}$ process.

Product ID	ESI(+)MS m/z	ESI(+)MS2 m/z	UV absorbance (λ_{\max})	Proposed structure
1	196	196	219, 252	
2	224	224, 196	219, 255	
3	267, 249	249, 239, 224, 196	225, 241, 312	
4	267	249, 224	227, 272, 345	
5	253	253, 236, 210, 180	219, 238, 279	
6	285, 267	267, 239, 224, 196	224, 263, 321	
7	287	287, 253, 236, 223, 196, 180	220	
8	271	253, 210	221	
9	283	265, 240, 222, 196	224, 313	

Table 1 (Continued)

Product ID	ESI(+)MS <i>m/z</i>	ESI(+)MS2 <i>m/z</i>	UV absorbance (λ_{\max})	Proposed structure
10	267	249, 221	226, 272, 348	
11	271	253, 210, 180	219	
12	180	180	211, 249	
13*	193, 165			

The intermediate marked with * is identified by SPME/GC/MS).

ratio of $[S_2O_8^{2-}]:[Fe^{3+}]:[CBZ] = 40:5:1$ at pH 3, and only 24% of CBZ was removed after 40 min (data not shown).

3.5. Effect of various inorganic anions

CBZ may co-exist with various inorganic ions in some waters such as sea water. Previous studies reported that the presence of some inorganic ions could affect the degradation of organic compounds in the sulfate radicals-based advanced oxidation process [25,32,33]. Xu and Li observed the presence of Cl^- , NO_3^- , HCO_3^- and $H_2PO_4^-$ had a noticeably negative effect on the decomposition of azo dye orange G by $Fe^{2+}/S_2O_8^{2-}$ process [25]. It was reported that Cl^- and HCO_3^- exerted no influence on the degradation of *p*-nitrosodimethylaniline by $Fe^{2+}/S_2O_8^{2-}$ process with the presence of chelate (citric acid) under neutral conditions while Cl^- significantly inhibited the degradation of perchloroethylene by $Fe^{2+}/S_2O_8^{2-}$ process at pH 2 [33]. This study evaluated the influence of four inorganic anions, including Cl^- , NO_3^- , SO_4^{2-} and $H_2PO_4^-$ on the performance of $Fe^{2+}/S_2O_8^{2-}$ system in terms of CBZ decay. As shown in Fig. 5, the addition of 0.01 M Cl^- remarkably accelerated CBZ degradation, where 100% removal efficiency of CBZ was observed in 5 min (before the first sample was taken). Wang and Chu also reported chloride ions exerted a positive influence on the degradation of Rhodamine B under acidic conditions in $Fe^{2+}/Oxone$ system [32]. The NO_3^- , SO_4^{2-} and $H_2PO_4^-$ however inhibited CBZ decay in the ascending order of $NO_3^- < SO_4^{2-} < H_2PO_4^-$. The inhibiting effect of NO_3^- and SO_4^{2-} may be because the high ion strength, which resulted in a slower decomposition of persulfate ions [34,35]. In addition, the presence of SO_4^{2-} will reduce of half-reaction reduction potential of sulfate radical ($E^{\theta}_{(SO_4^{2-}/SO_4^{2-})}$) [32]. $H_2PO_4^-$ might form complexes with iron species in aqueous media. Thus, Fe^{2+} is not free to react with PS in the solution [36].

It is interesting to observe the positive effect of chloride, additional tests were conducted as shown in Fig. 6. The first-stage decay rate of CBZ increased with the increment of $[Cl^-]$. The removal efficiency of CBZ was nearly 99% after 1 min of reaction in the presence of 10 mM Cl^- , while only around 60% of CBZ was eliminated after 10 min in a chloride-free solution. The accelerating effect of Cl^- was

also reported in the degradation of Rhodamin B by $Fe^{2+}/Oxone$ [32], in which the chloride ion could improve the dye degradation even in the absence of Fe^{2+} ; this however was not observed in this study. The positive role of Cl^- on the reaction performance of CBZ degradation may be due to the generation of the additional radicals such as Cl^{\bullet} and $Cl_2^{\bullet-}$ through a series of chain reactions (Eq. (9)–(14)) [27].



However, the negative effect of Cl^- was also found on the degradation of the azo dye Orange G and perchloroethylene [25,33]. In $SO_4^{\bullet-}$ -based advanced oxidation processes, the different role of Cl^- in the decomposition of the azo dye Orange G and CBZ may be attributed to their different molecular structure. The molecular structure of CBZ contains an olefinic double bond which is susceptible to the attack of chlorine radicals. Wang and Chu observed the degradation of Rhodamine B in the co-existence of Oxone and chloride without Fe^{2+} , which was ascribe to the generation of HOCl in Eqs. (15) and (16).



From a thermodynamic point of view, $S_2O_8^{2-}$ ($E^0 = 2.01$ V) [25] could also oxidize Cl^- to form chlorine ($Cl_2/Cl^-, 1.36$ V) and hypochlorous acid ($HOCl/Cl^-, 1.48$ V) [27,37]. The CBZ decay was

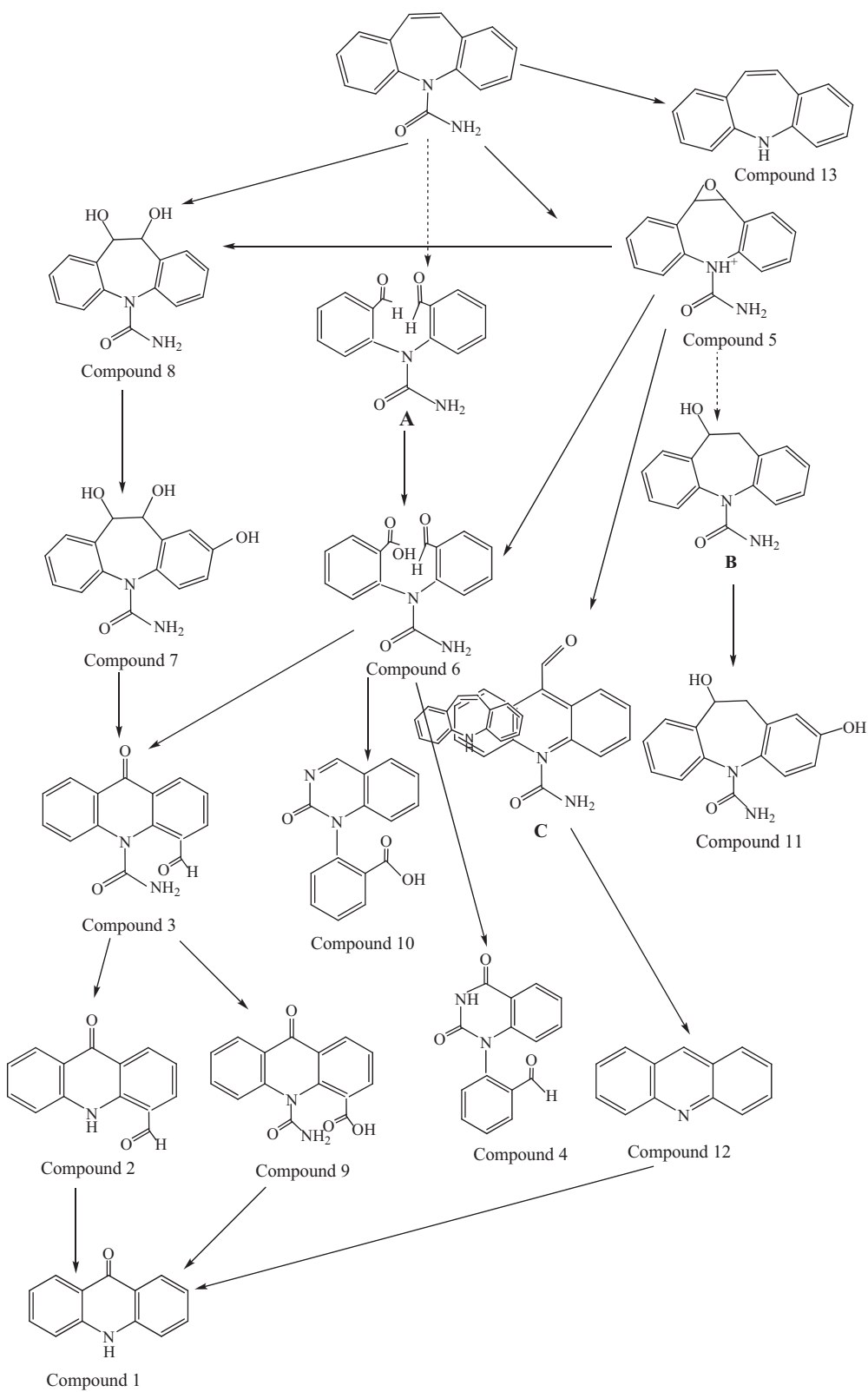


Fig. 8. Proposed decay pathways of CBZ by $\text{Fe}^{2+}/\text{S}_2\text{O}_8^{2-}$ process.

not observed in the co-existence of $\text{S}_2\text{O}_8^{2-}$ and chloride in the absence of Fe^{2+} , which is because both Cl_2 and HOCl are not capable of oxidizing CBZ. Although Cl^- plays a positive role in CBZ degradation by $\text{Fe}^{2+}/\text{S}_2\text{O}_8^{2-}$ process, the presence of Cl^- may introduce unfavorable chlorinated intermediates/products, which will be discussed further in the next section.

3.6. Identification and evolution of intermediates and products

To reveal the detail about Cl^- influence on CBZ degradation, the identification of the intermediates and the investigation on the evolution of intermediates generated during CBZ decomposition by $\text{Fe}^{2+}/\text{S}_2\text{O}_8^{2-}$ process with and without Cl^- was conducted.

During CBZ degradation with and without Cl^- , the same 12 intermediates were detected by LC-MS/MS and one intermediate was identified by SPME/GC/MS (See Table 1). Molecular structures were proposed for each intermediate/product on the basis of the molecular ion masses and MS2 fragmentation patterns (MS2 spectra for each intermediate/product provided in the Supporting information). Among the intermediates, there are five isomers (compounds 3, 4 and 10; compounds 8 and 11). It is not difficult to identify compounds 3, 4 and 10 since they demonstrate different MS2 fragmentation patterns. The proposed structures of these three isomers are in accordance with previous studies [13,38]. However, compounds 8 and 11 show similar MS2 fragmentation patterns. The identification of these two isomers is based on their yields. Compared to the two outside benzene rings, the olefinic double bond on the central heterocyclic ring shows higher reactivity towards electrophilic attack by radicals, leading to higher yields of the intermediates/products from the electrophilic attack at the olefinic double bond than that of other intermediates/products from other pathways. Since the yield of compound 8 is higher than that of compound 11, compound 8 is assigned as 10,11-dihydro-dihydroxycarbamazepine. Compound 11 is attributed to 10,11-dihydro-2,10-dihydroxycarbamazepine. The identity of compound 5 was confirmed by comparing its retention time and mass fragmentation pattern to that of the authentic compound (Carbamazepine 10, 11-epoxide). Compounds 6 and 7 are believed to come from the further oxidation of compound 8. Compounds 1, 2, 3 and 9 are believed to derive from cyclization reaction [39] and their structures have been proposed in previous contributions [38,40]. Compound 12 was identified by both LC/MS/MS and GC/MS while compound 13 was identified by GC/MS. The evolution profiles of the major intermediates/products were organized and shown in Fig. 7a and b (trace intermediates/products not included). CBZ degradation and TOC removal efficiency were also illustrated in Fig. 7a and b. More than 90% CBZ removal was achieved in 5 min with the presence of Cl^- , while CBZ removal was merely 47.3% after 40 min without Cl^- . After 40 min of reaction, TOC removal efficiency with Cl^- (14.6%) is higher than that without Cl^- (8%). Due to the presence of Cl^- leading to the generation of other radicals such as $\text{Cl}\cdot$ and $\text{Cl}_2\cdot$, the formation/degradation profiles of some intermediates/products generated during CBZ degradation by $\text{Fe}^{2+}/\text{S}_2\text{O}_8^{2-}$ with and without the presence of Cl^- are different as shown in Fig. 7a and b. The yield of compound 2 and 6 is the highest without and with Cl^- , respectively. CBZ decomposition generated trace compound 3 without Cl^- while the accumulation of compound 5 was not observed with Cl^- . The yield of compound 11 is lower than that of compounds 2, 5, 6, 8 and 9. On the other hand, the generation of compound 11 is higher than compounds 2, 5, 8 and 9. Compound 13 was identified by GC/MS. Anipsitakis et al. reported that sulfate radicals attack on phenolic compounds in the presence of chloride led to the generation of chlorinated phenolic compounds [27]. However, chlorinated intermediates/products were not detected with the presence of chloride in this study. This may be due to the use of low initial concentration (0.15 mM) of CBZ, which is much lower than that in Anipsitakis's study (655.8 mM Phenol). Thus, no chlorinated intermediates/products can accumulate to an appreciable level.

3.7. Proposed CBZ degradation pathways

Reaction pathways for CBZ degradation by $\text{Fe}^{2+}/\text{S}_2\text{O}_8^{2-}$ process are proposed in Fig. 8. Four primary intermediates (Compounds 5, 6, 8 and 13) were generated upon CBZ's degradation, which were initiated by electrophilic attack at the olefinic double bond on the central heterocyclic ring by sulfate radicals or hydroxyl radicals. At the initial stage, the two benzene rings remain intact. The addition of radicals to the olefinic double bond of CBZ could

generate an epoxide (compound 5). The addition of radicals to the olefinic double bond in pairs produced a saturated glycols (compound 8). Hydroxyl radical is also capable of reacting with olefinic double bond by oxidizing/breaking the double bond and generating two aldehydes or ketones, such as compound A (not detected though). However, compound 6 is believed to derive from the further oxidation of compound A. In addition, compounds 6 and 8 might not directly come from CBZ but from compound 5. To verify this, compound 5 was used as the starting probe in $\text{Fe}^{2+}/\text{S}_2\text{O}_8^{2-}$ process as an independent test, where both compounds 6 and 8 were detected. Thus, compounds 6 and 8 could be primary and secondary intermediates. The loss of amide group of CBZ led to the generation of compound 13. Compound 11 is believed to derive from compound 5 through the attack at the benzene ring of "intermediate B" by sulfate radicals. The radical attack tends to happen on carbon 2 and carbon 4 on the benzene ring due to the electron-donating property of the nitrogen group on the central heterocyclic ring. Owing to steric effect, the radical attack prefers taking place on carbon 2 (para-position), leading to the generation of compound 11. Ring contraction of compound 5 would possibly involve the formation of "intermediate C (carbamazepine-9-carboxaldehyde)" as reported in other studies [41]. The succeeding losses of carboxyaldehyde group and CONH_2 lateral chain of "intermediate C" might yield compound 12. Compound 7 is believed to derive from compound 8 via the attack at the carbon 2 on the benzene ring by hydroxyl radicals. Compound 6 might evolve in three different ways: (1) Intramolecular cyclization via electrophilic aromatic substitution to generate compound 3; (2) The ring closure proceeds through intramolecular attack by nitrogen at the aldehyde, leading to the production of compound 10; and (3) Intramolecular attack by hydrogen-carrying nitrogen at the carbonyl giving compound 4. The evolution of compound 3 may proceed in two different ways: (1) the hydrolysis of the urea group on the central heterocyclic ring leading to compound 2; and (2) the aldehyde group on the benzene ring being further oxidized to produce compound 9. Compound 1 might arise from three sources: (1) the loss of carboxyaldehyde group on the benzene ring of compound 2; (2) succeeding losses of carboxyl and CONH_2 lateral chain of compound 9; and (3) the oxidation of compound 12.

4. Conclusions

The degradation of CBZ was investigated using sulfate radicals generated by the coupling of ferrous ions and persulfate as transition metal and oxidant, respectively. CBZ decay can be described as a two-stage reaction consisting of a rapid initial stage followed by a retarded second stage. Experimental results also show that the performance of CBZ degradation was influenced by operating parameters, such as the molar ratio and the concentration of Fe^{2+} and $\text{S}_2\text{O}_8^{2-}$, initial solution pH, and inorganic salts. Optimum CBZ removal efficiency was observed at an initial solution pH of 3.0 within the investigated pH range of 2.00–7.87. Optimum molar ratio of $\text{Fe}^{2+}/\text{S}_2\text{O}_8^{2-}/\text{CBZ}$ was identified to be 5:40:1. The presence of certain anions had a significant effect on the $\text{Fe}^{2+}/\text{S}_2\text{O}_8^{2-}$ process. It was found that NO_3^- , SO_4^{2-} and H_2PO_4^- demonstrated adverse effects (in an ascending order) on CBZ decay in the process. The existence of Cl^- however facilitated the decomposition of CBZ, where the higher Cl^- concentration, the faster CBZ decay rate. In addition, 13 intermediates were identified during CBZ degradation by $\text{Fe}^{2+}/\text{S}_2\text{O}_8^{2-}$ process with and without the presence of Cl^- . The evolution profiles of intermediates are different for these two scenarios. Based on the analysis of the evolution profiles of intermediates, the decay pathways were proposed accordingly.

References

- [1] B. Halling-Sorensen, S.N. Nielsen, P.F. Lanzky, F. Ingerslev, H.C.H. Lutzhoft, S.E. Jorgensen, Occurrence, fate and effects of pharmaceutical substances in the environment—a review, *Chemosphere* 36 (1998) 357–394.
- [2] Y.J. Zhang, S.U. Geissen, C. Gal, Carbamazepine and diclofenac: removal in wastewater treatment plants and occurrence in water bodies, *Chemosphere* 73 (2008) 1151–1161.
- [3] CMEIN, Chinese Medical Statistical Yearbook, CMEIN, Products Section, Beijing, China, 2005.
- [4] T.A. Ternes, Occurrence of drugs in German sewage treatment plants and rivers, *Water Res.* 32 (1998) 3245–3260.
- [5] T. Heberer, Tracking persistent pharmaceutical residues from municipal sewage to drinking water, *J. Hydrol.* 266 (2002) 175–189.
- [6] A. Ginebreda, I. Munoz, M. Lopez de Alda, R. Brix, J. Lopez-Doval, D. Barcelo, Environmental risk assessment of pharmaceuticals in rivers: relationships between hazard indexes and aquatic macroinvertebrate diversity indexes in the Llobregat River (NE Spain), *Environ. Int.* 36 (2010) 153–162.
- [7] J.E. Drewes, T. Heberer, K. Reddersen, Fate of pharmaceuticals during indirect potable reuse, *Water Sci. Technol.* 46 (2002) 73–80.
- [8] T. Heberer, K. Reddersen, A. Mechlinski, From municipal sewage to drinking water: fate and removal of pharmaceutical residues in the aquatic environment in urban areas, *Water Sci. Technol.* 46 (2002) 81–88.
- [9] B. Ferrari, N. Paxeus, R. Lo Giudice, A. Pollio, J. Garric, Ecotoxicological impact of pharmaceuticals found in treated wastewaters: study of carbamazepine, clofibric acid, and diclofenac, *Ecotox. Environ. Saf.* 55 (2003) 359–370.
- [10] Z.H. Li, V. Zlabek, J. Velisek, R. Grabic, J. Machova, J. Kolarova, P. Li, T. Randak, Acute toxicity of carbamazepine to juvenile rainbow trout (*Oncorhynchus mykiss*): effects on antioxidant responses, hematological parameters and hepatic EROD, *Ecotox. Environ. Saf.* 74 (2011) 319–327.
- [11] T.E. Doll, F.H. Frimmel, Photocatalytic degradation of carbamazepine, clofibric acid and iomeprol with P25 and Hombikat UV100 in the presence of natural organic matter (NOM) and other organic water constituents, *Water Res.* 39 (2005) 403–411.
- [12] C. Martinez, M. Canle, M.J. Fernandez, J.A. Santaballa, J. Faria, Kinetics and mechanism of aqueous degradation of carbamazepine by heterogeneous photocatalysis using nanocrystalline TiO₂, ZnO and multi-walled carbon nanotubes-anatase composites, *Appl. Catal., B* 102 (2011) 563–571.
- [13] D.C. McDowell, M.M. Huber, M. Wagner, U. Von Gunten, T.A. Ternes, Ozonation of carbamazepine in drinking water: identification and kinetic study of major oxidation products, *Environ. Sci. Technol.* 39 (2005) 8014–8022.
- [14] A. Ghauch, H. Baydoun, P. Dermesopian, Degradation of aqueous carbamazepine in ultrasonic/Fe⁰/H₂O₂ systems, *Chem. Eng. J.* 172 (2011) 18–27.
- [15] C.M. Dai, X.F. Zhou, Y.L. Zhang, Y.P. Duan, Z.M. Qiang, T.C. Zhang, Comparative study of the degradation of carbamazepine in water by advanced oxidation processes, *Environ. Technol.* 33 (2012) 1101–1109.
- [16] G.P. Anipsitakis, D.D. Dionysiou, Degradation of organic contaminants in water with sulfate radicals generated by the conjunction of peroxymonosulfate with cobalt, *Environ. Sci. Technol.* 37 (2003) 4790–4797.
- [17] T.K. Lau, W. Chu, N.J.D. Graham, The aqueous degradation of butylated hydroxyanisole by UV/S₂O₈²⁻: study of reaction mechanisms via dimerization and mineralization, *Environ. Sci. Technol.* 41 (2007) 613–619.
- [18] K.H. Chan, W. Chu, Degradation of atrazine by cobalt-mediated activation of peroxymonosulfate: different cobalt counteranions in homogenous process and cobalt oxide catalysts in photolytic heterogeneous process, *Water Res.* 43 (2009) 2513–2521.
- [19] J.E.B. McCallum, S.A. Madison, S. Alkan, R.L. Depinto, R.U.R. Wahl, Analytical studies on the oxidative degradation of the reactive textile dye Uniblue A, *Environ. Sci. Technol.* 34 (2000) 5157–5164.
- [20] A. Ghauch, A.M. Tuqan, N. Kibbi, Ibuprofen removal by heated persulfate in aqueous solution: a kinetics study, *Chem. Eng. J.* 197 (2012) 483–492.
- [21] T. Olmez-Hanci, I. Arslan-Alaton, B. Genc, Bisphenol A treatment by the hot persulfate process: oxidation products and acute toxicity, *J. Hazard. Mater.* 263 (Pt 2) (2013) 283–290.
- [22] L. Bingzhi, L. Lin, L. Kuangfei, Z. Wei, L. Shuguang, L. Qishi, Removal of 1,1,1-trichloroethane from aqueous solution by a sono-activated persulfate process, *Ultrason. Sonochem.* 20 (2013) 855–863.
- [23] Y. Lee, S. Lo, J. Kuo, C. Hsieh, Decomposition of perfluoroctanoic acid by microwaveactivated persulfate: effects of temperature, pH, and chloride ions, *Front. Environ. Sci. Eng.* 6 (2012) 17–25.
- [24] L. Zhou, W. Zheng, Y. Ji, J. Zhang, C. Zeng, Y. Zhang, Q. Wang, X. Yang, Ferrous-activated persulfate oxidation of arsenic(III) and diuron in aquatic system, *J. Hazard. Mater.* 263 (Pt 2) (2013) 422–430.
- [25] X.R. Xu, X.Z. Li, Degradation of azo dye Orange G in aqueous solutions by persulfate with ferrous ion, *Sep. Purif. Technol.* 72 (2010) 105–111.
- [26] G.P. Anipsitakis, D.D. Dionysiou, Radical generation by the interaction of transition metals with common oxidants, *Environ. Sci. Technol.* 38 (2004) 3705–3712.
- [27] G.P. Anipsitakis, D.D. Dionysiou, M.A. Gonzalez, Cobalt-mediated activation of peroxymonosulfate and sulfate radical attack on phenolic compounds: implications of chloride ions, *Environ. Sci. Technol.* 40 (2006) 1000–1007.
- [28] C.F.H.C. Liang, N. Mohanty, R.M. Kurakalva, A rapid spectrophotometric determination of persulfate anion in ISCO, *Chemosphere* 73 (2008) 1540–1543.
- [29] N. Masompoon, C. Ratanatamskul, M.-C. Lu, Chemical oxidation of 2,6-dimethylaniline in the Fenton process, *Environ. Sci. Technol.* 43 (2009) 8629–8634.
- [30] O.A.H. Jones, N. Voulvoulis, J.N. Lester, Aquatic environmental assessment of the top 25 English prescription pharmaceuticals, *Water Res.* 36 (2002) 5013–5022.
- [31] A. Stefansson, Iron(III) hydrolysis and solubility at 25 °C, *Environ. Sci. Technol.* 41 (2007) 6117–6123.
- [32] Y.R. Wang, W. Chu, Degradation of a xanthene dye by Fe(II)-mediated activation of Oxone process, *J. Hazard. Mater.* 186 (2011) 1455–1461.
- [33] L.R. Bennedsen, J. Muff, E.G. Sogaard, Influence of chloride and carbonates on the reactivity of activated persulfate, *Chemosphere* 86 (2012) 1092–1097.
- [34] I.M. Kolthoff, I.K. Miller, The kinetics and mechanism of the decomposition of the persulfate ion in aqueous medium, *J. Am. Chem. Soc.* 73 (1951) 3055–3059.
- [35] K.C. Huang, A.C. Richard, E.H. George, Kinetics of heat-assisted persulfate oxidation of methyl *tert*-butyl ether (MTBE), *Chemosphere* 49 (2002) 413–420.
- [36] G.A.A. Ghauch, S. Naim, Degradation of sulfamethoxazole by persulfate assisted micrometric Fe⁰ in aqueous solution, *Chem. Eng. J.* 228 (2013) 1168–1181.
- [37] E.T. Urbansky, Total organic carbon analyzers as tools for measuring carbonaceous matter in natural waters, *J. Environ. Monitor.* 3 (2001) 102–112.
- [38] L. Hu, H.M. Martin, O. Arcs-Bulted, M.N. Sugihara, K.A. Keatng, T.J. Strathmann, Oxidation of carbamazepine by Mn(VII) and Fe(VI): reaction kinetics and mechanism, *Environ. Sci. Technol.* 43 (2009) 509–515.
- [39] K. Dzierbicka, A.M. Kolodziejczyk, Synthesis and antitumor activity of conjugates of muramyldipeptide or normuramyldipeptide with hydroxyacridine/acridone derivatives, *J. Med. Chem.* 46 (2003) 183–189.
- [40] S. Chiron, C. Minero, D. Vione, Photodegradation processes of the antiepileptic drug carbamazepine, relevant to estuarine waters, *Environ. Sci. Technol.* 40 (2006) 5977–5983.
- [41] D. Vogna, R. Marotta, R. Andreozzi, A. Napolitano, M. d'Ischia, Kinetic and chemical assessment of the UV/H₂O₂ treatment of antiepileptic drug carbamazepine, *Chemosphere* 54 (2004) 497–505.